The 8th European Congress on Computational Methods in Applied Sciences and Engineering
ECCOMAS Congress 2022
5-9 June 2022, Oslo, Norway

A VARIATIONAL-BASED MIXED FINITE ELEMENT FORMULATION FOR LIQUID CRYSTAL ELASTOMERS

Michael Groß[1], Julian Dietzsch[2] and Francesca Concas[3]

[1] TU Chemnitz, Reichenhainer Straße 70, D-09126 Chemnitz,
michael.gross@mb.tu-chemnitz.de,
[2] julian.dietzsch@mb.tu-chemnitz.de,
[3] francesca.concas@mb.tu-chemnitz.de.

Keywords: *Anisotropy, Finite Element Method, Variational Principle, Mixed Method.*

Abstract. Liquid crystal elastomers (LCEs) are soft materials, which are capable of large deformations induced by temperature changes and ultraviolet irradiation [1]. Since many years, these materials are under investigation in experimental researches as actuator materials. LCEs arise from a nematic polymer melt, consisting of long and flexible polymer chains as well as oriented and rigid rod-like molecules, the so-called mesogens, by crosslinking. In order to numerically simulate LCE materials by using the finite element method, a continuum model is necessary, including in a thermo-viscoelastic material formulation of the polymer chains the orientation effects of the mesogens. This can be performed by introducing a normalized direction vector as an independent field, and deriving from additional (orientational) balance laws independent differential equations [2]. These differential equations describe the independent rotation of the rigid mesogens connected with the flexible polymer chains. The orientation-dependent stress law of LCEs arises from an anisotropic free energy, comparable with fibre-reinforced materials. But, in contrast to fibre-reinforced materials, the direction vector of a LCE model has to be independent. In contrast to [2], we apply a variational principle for deriving a new mixed finite element formulation, which is based on drilling degrees of freedom for describing the mesogens rotation [3]. This principle leads to an extended set of balance laws.

1 INTRODUCTION

1.1 Preliminaries

Amorphous polymers are exceptionally deformable irregular networks of long molecule chains. On the other hand, liquid crystals are liquids with regularly arranged or oriented molecules. Since this is not a crystal phase nor an isotropic liquid phase, liquid crystals are anisotropic liquids in the so-called mesophase. If these molecules have a pronounced anisotropic shape as a rod, the molecules are called *mesogens*. Polymer chains can be linked with mesogens by means of chemical reactions to a liquid crystal elastomer (LCE) network. The simplest form of a mesophase is the nematic phase, because here the longitudinal axes of the rod-like mesogens are arranged almost in parallel. If liquid crystals are linked to the polymer chains in the nematic phase, there results a nematic LCE.
In nematic liquid crystalline elastomers, a temperature increase leads to a rotation of

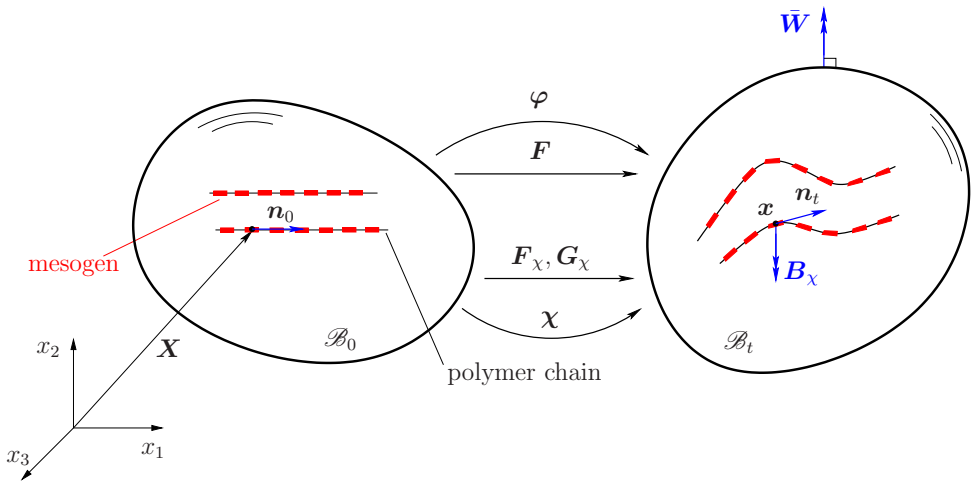

Figure 1: Continuum configurations of a LCE with orientational volume and surface loads.

the mesogens. This leads to a contraction of the LCE material (see Fig. 2 in [1]). The mesogens in a nematic LCE can be described by an orientation vector $\boldsymbol{n}_0$, with $\boldsymbol{n}_0 \cdot \boldsymbol{n}_0 = 1$ (see Fig. 1), in the nematic initial configuration $\mathscr{B}_0$. Hence, the temperature increase causes the rotation of the orientation vector at the material point $\boldsymbol{X} \in \mathscr{B}_0$ into the orientation vector $\boldsymbol{n}_t$ at point $\boldsymbol{x} \in \mathscr{B}_t$ of the current configuration $\mathscr{B}_t$ (see Fig. 3 in [1]). During the crosslinking reaction, rod-like dye molecules as azobenzene can be introduced as a third component. These materials are called azo-dye-doped nematic LCE materials. The azobenzene molecules can be transferred from the elongated 'trans' shape in the angled 'cis' shape, and vice versa, by irradiation with ultraviolet light (see Fig. 9 in [1]).

1.2 Motivation and goals

First constitutive laws for liquid crystals are presented in Reference [4], wherein a free energy function in dependence on the orientation vector $\boldsymbol{n}_t$ is derived. This Frank free energy increases with the distorsion of the orientation vector field $\boldsymbol{n}_t(\boldsymbol{x})$. It is based on a quadratic form with respect to the spatial gradient grad$[\boldsymbol{n}_t]$, where grad$[\bullet]$ denotes the partial derivative with respect to $\boldsymbol{x} \in \mathscr{B}_t$.
Reference [5] is a first one about a continuum theory for LCE, in which $\boldsymbol{n}_t$ is considered as a global, independent field with boundary conditions. This theory defines balance laws with an additional kinetic energy with respect to the partial time derivative $\dot{\boldsymbol{n}}_t$ as well as mechanical power of volume and surface forces acting on $\boldsymbol{n}_t$. In this way, the linear momentum balance law defines the motion of the LCE, and an orientational momentum balance law the time evolution of $\boldsymbol{n}_t$.
In Reference [2], this approach is extended by the dynamical constraint $\boldsymbol{n}_t \cdot \boldsymbol{n}_t = 1$ in the sense of a differential-algebraic system. Here, the balance laws are formulated in a Lagrangian description in dependence of the material gradient Grad$[\boldsymbol{n}_t \circ \boldsymbol{\varphi}]$, where Grad$[\bullet]$ denotes the partial derivative with respect to $\boldsymbol{X} \in \mathscr{B}_0$ and $\boldsymbol{\varphi}$ indicates the deformation mapping (see Fig. 1). In this work, the free energy includes the Frank free energy. Reference [6] satisfies the dynamical constraint $\|\boldsymbol{n}_t\| = 1$ by means of a second-order rotation tensor. However, in this way, the balance equation for the direction vector $\boldsymbol{n}_t$ takes the form of a matrix equation.
LCE materials are suitable for contactless actuator components for integration into light-weight structures. The development of such actuated light-weight structures can be per-

formed numerically by dynamic finite element methods, if an appropriate mathematical formulation of the constitutive laws and the time evolution equations is used. Since the LCE materials are usely thin structures, a locking-free mixed finite element formulation is recommendable. A special mixed finite element formulation with the orientation vector $\boldsymbol{n}_t$ as independent field is also able to avoid a differential-algebraic equation system or a rotation tensor equation, respectively, to obtain a normalized orientation vector $\boldsymbol{n}_t$ at each time. More precisely, the pure rotation of the orientation vector $\boldsymbol{n}_t$ can be formulated by local drilling degrees of freedom as in Reference [3]. In order to simulate high-frequent oscillations of LCE actuators efficiently (see Figs. 24 and 25 in [1]), numerically stable time integrators based on variational principles are also recommended.
Therefore, in this paper, we present as a point of departure an isothermal variational-based mixed finite element formulation with (i) drilling degrees of freedom in order to rotate the orientation vector, (ii) locking-free mixed finite elements, and (iii) a numerically stable variational-based Galerkin time integration. This mixed finite element formulation satisfies a number of balance laws numerically exactly during a stable LCE simulation.

2 MIXED FINITE ELEMENT FORMULATION

2.1 Continuum model

We consider the LCE material as a n_{dim}-dimensional continuum in the configuration $\mathscr{B}_0 \subset \mathbb{R}^{n_{\text{dim}}}$ with the orientation vector $\boldsymbol{n}_0(\boldsymbol{X})$ in the material point $\boldsymbol{X} \in \mathscr{B}_0$ at initial time $t = 0$. The *deformation mapping* $\boldsymbol{\varphi} : \mathscr{B}_0 \times \mathscr{T} \to \mathscr{B}_t$ describes the motion in the time interval $\mathscr{T} = [0, T]$ of the LCE material into the deformed configuration $\mathscr{B}_t$ at time $t \in \mathscr{T}$, and satisfies the identity $\boldsymbol{\varphi}(\boldsymbol{X}, 0) = \boldsymbol{X}$ at each $\boldsymbol{X} \in \mathscr{B}_0$. The *orientation mapping*

$$\boldsymbol{\chi} : \mathscr{B}_0 \times \mathscr{T} \to \mathbb{R}^{n_{\text{dim}}} \quad \text{, satisfying} \quad \boldsymbol{\chi}(\boldsymbol{X}, 0) = \boldsymbol{n}_0(\boldsymbol{X}) \tag{1}$$

at each point $\boldsymbol{X} \in \mathscr{B}_0$, gives the orientation vector $\boldsymbol{n}_t(\boldsymbol{x})$ in the material point $\boldsymbol{x} \in \mathscr{B}_t$. The deformation mapping results by time integration from the *material velocity vector* $\boldsymbol{v}(\boldsymbol{X}, t) := \dot{\boldsymbol{\varphi}}(\boldsymbol{X}, t) = \dot{\boldsymbol{x}}$, where the superposed dot denotes the partial derivative with respect to time t. The orientation mapping arises from the *orientational velocity vector*

$$\boldsymbol{v}_\chi(\boldsymbol{X}, t) := \dot{\boldsymbol{\chi}}(\boldsymbol{X}, t) = \dot{\boldsymbol{n}}_t \tag{2}$$

By denoting with ρ_0 the mass density of the LCE material in the initial configuration $\mathscr{B}_0$, we obtain the linear momentum vector $\boldsymbol{p} := \rho_0 \, \boldsymbol{v}$. In accordance with References [2, 3], we assume a *radius of gyration* l_χ associated with the molecule in direction $\boldsymbol{n}_0$ within the representative volume element of the edge length l_0 at each material point $\boldsymbol{X} \in \mathscr{B}_0$. In this way, we arrive at the *orientational momentum vector*

$$\boldsymbol{p}_\chi := \rho_0 \left[(l_\chi^2 - l_0^2) \boldsymbol{A}_0 + l_0^2 \, \boldsymbol{I} \right] \boldsymbol{v}_\chi \tag{3}$$

where $\boldsymbol{A}_0 := \boldsymbol{n}_0 \otimes \boldsymbol{n}_0$ denotes the second-order *structural tensor* of the mesophase and $\boldsymbol{I}$ the second-order identity tensor. During the motion, the infinitesimal line element $\mathrm{d}\boldsymbol{x} = \boldsymbol{F} \, \mathrm{d}\boldsymbol{X}$ at the position $\boldsymbol{x} \in \mathscr{B}_t$ is given by the deformation gradient $\boldsymbol{F} := \mathrm{Grad}[\boldsymbol{\varphi}]$. Analogously, we introduce the *orientation tensor* $\boldsymbol{F}_\chi := \boldsymbol{\chi} \otimes \boldsymbol{n}_0$, which maps the initial orientation $\boldsymbol{n}_0$ to the current orientation $\boldsymbol{n}_t$ (see Fig. 1). Hence, we obain the relation

$$\boldsymbol{n}_t = \boldsymbol{F}_\chi \, \boldsymbol{n}_0 \tag{4}$$

The stretch of the material line element $\mathrm{d}\boldsymbol{x}$ during a deformation is measured by the right Cauchy-Green tensor $\boldsymbol{C} := \boldsymbol{F}^t\,\boldsymbol{g}\,\boldsymbol{F}$ with respect to the *translational metric tensor* $\boldsymbol{g} := \mathrm{grad}[\boldsymbol{x}]$. We denote by the superscript t the transposition of a second-order tensor. In the same way, the stretch of the material line element $\mathrm{d}\boldsymbol{x}$ due to the rotation of the orientation vector $\boldsymbol{n}_t$ is determined by the *orientational deformation tensor*

$$\boldsymbol{C}_\chi := \boldsymbol{F}^t\,\boldsymbol{g}\,\boldsymbol{F}_\chi \equiv \boldsymbol{F}^t\,\boldsymbol{g}_\chi\,\boldsymbol{F} \tag{5}$$

where $\boldsymbol{g}_\chi$ designates the *orientational metric tensor*. Note that we indicate by the index χ the correspondence to the orientation mapping $\boldsymbol{\chi}$.

Remark 2.1 *Assuming curvilinear covariant basis vectors $\boldsymbol{G}_i$, $i = 1,\dots,n_{\mathrm{dim}}$, in the initial configuration $\mathscr{B}_0$, and contravariant basis vectors $\boldsymbol{g}^i$ in the current configuration $\mathscr{B}_t$, the metric tensor $\boldsymbol{g}_\chi := \mathfrak{g}_i \otimes \boldsymbol{g}^i$ (summation convention is implied) belongs to the orientational covariant basis vectors $\mathfrak{g}_i := \boldsymbol{F}_\chi\,\boldsymbol{G}_i$. The covariant basis vectors $\boldsymbol{g}_i$ also defines the translational metric tensor $\boldsymbol{g} := \boldsymbol{g}_i \otimes \boldsymbol{g}^i$. In this notation, the deformation gradient is given by $\boldsymbol{F} := \boldsymbol{g}_i \otimes \boldsymbol{G}^i$ and the orientation tensor reads $\boldsymbol{F}_\chi := \mathfrak{g}_i \otimes \boldsymbol{G}^i$ with respect to the contravariant basis vectors $\boldsymbol{G}^i$ associated with the initial configuration $\mathscr{B}_0$. The translational metric tensor $\boldsymbol{G} := \boldsymbol{G}_i \otimes \boldsymbol{G}^i$ then belongs to the initial configuration.*

The orientational invariants in Reference [2] for describing the *interactive free energy density* $\Psi_i(\boldsymbol{F}^t\,\boldsymbol{g}\,\boldsymbol{\chi}) := \hat{\Psi}^{\mathrm{ori}}(I_1^{\mathrm{ori}}, J_2^{\mathrm{ori}})$ can be then written as

$$I_1^{\mathrm{ori}} := \boldsymbol{C}_\chi \boldsymbol{A}_0 : \boldsymbol{G}^{-1} \qquad J_2^{\mathrm{ori}} := \boldsymbol{C}_\chi \boldsymbol{A}_0 : \boldsymbol{C}_\chi \boldsymbol{A}_0 \tag{6}$$

where the symbol : indicates double contraction. Hence, we consider the interactive free energy $\Psi^{\mathrm{ori}}(\boldsymbol{C}_\chi)$. The *elastic free energy density* $\Psi^{\mathrm{ela}}(\boldsymbol{C}) := \hat{\Psi}^{\mathrm{ela}}(I_1^{\mathrm{ela}}, J_2^{\mathrm{ela}}, I_3^{\mathrm{ela}})$ in Reference [2] associated with an isotropic material depends on the invariants

$$I_1^{\mathrm{ela}} := \boldsymbol{C} : \boldsymbol{G}^{-1} \qquad J_2^{\mathrm{ela}} := \boldsymbol{C} : \boldsymbol{C} \qquad I_3^{\mathrm{ela}} := \det[\boldsymbol{C}] \tag{7}$$

In order to quantify the increase of the Frank free energy density caused by distorsions from the uniformly aligned initial configuration $\mathscr{B}_0$, we introduce the *distorsion tensor*

$$\boldsymbol{K}_\chi := \boldsymbol{F}^t\,\boldsymbol{g}\,\boldsymbol{G}_\chi = \boldsymbol{F}^t\,\boldsymbol{g}_K\,\boldsymbol{F} \tag{8}$$

with the metric tensor $\boldsymbol{g}_K := \mathrm{grad}[\boldsymbol{n}_t]$. We refer to $\boldsymbol{G}_\chi := \mathrm{Grad}[\boldsymbol{\chi}]$ as the *orientation gradient*. Motivated by Reference [3], the distorsion can be then measured by the invariants

$$I_1^{\mathrm{dis}} := (\boldsymbol{K}_\chi - \mathrm{Grad}[\boldsymbol{n}_0]) : \boldsymbol{G}^{-1} \qquad J_2^{\mathrm{dis}} := (\boldsymbol{K}_\chi - \mathrm{Grad}[\boldsymbol{n}_0]) : (\boldsymbol{K}_\chi - \mathrm{Grad}[\boldsymbol{n}_0]) \tag{9}$$

which vanish in the initial configuration $\mathscr{B}_0$. Therefore, also simple constitutive laws as a quadratic St. Venant-Kirchhoff material may be applied as Frank free energy density $\Psi^{\mathrm{dis}}(\boldsymbol{K}_\chi)$. Accordingly, in this paper, the general form of the free energy reads

$$\boxed{\Psi(\boldsymbol{C}, \boldsymbol{C}_\chi, \boldsymbol{K}_\chi) := \Psi^{\mathrm{ela}}(\boldsymbol{C}) + \Psi^{\mathrm{ori}}(\boldsymbol{C}_\chi) + \Psi^{\mathrm{dis}}(\boldsymbol{K}_\chi)} \tag{10}$$

In a LCE material, the rotation of the orientation vector $\boldsymbol{n}_t$ is directly connected with the deformation of the polymer chain. Stretching the polymer chains, we obtain a stress field rotating the orientation vector. Such a dissipative *reorientation process* can be introduced

by a local evolution equation [7]. Analogous to finite viscoelasticity, we start with the Clausius-Planck inequality. Here, we obtain

$$D_\chi^{\text{int}} := \boldsymbol{N}_\chi : \boldsymbol{g}\,\dot{\boldsymbol{F}} - \dot{\Psi}^{\text{ori}}(\boldsymbol{C}_\chi) \equiv \left[\boldsymbol{N}_\chi - \boldsymbol{F}_\chi\,\boldsymbol{S}_\chi^t\right] : \boldsymbol{g}\,\dot{\boldsymbol{F}} - \boldsymbol{F}\,\boldsymbol{S}_\chi : \boldsymbol{g}\,\dot{\boldsymbol{F}}_\chi \geq 0 \tag{11}$$

as internal *reorientation dissipation* D_χ^{int}. From now on, we require that the orientation vector $\boldsymbol{n}_t$ has unit length $\|\boldsymbol{n}_t\| = 1$ at each time $t \in \mathscr{T}$. Hence, the velocity rate tensor $\boldsymbol{g}\,\dot{\boldsymbol{F}}_\chi\,\boldsymbol{F}_\chi^{-1}$ is skew-symmetric and can be written as

$$\mathbb{I}^{\text{skw}} : \boldsymbol{g}\,\dot{\boldsymbol{F}}_\chi\,\boldsymbol{F}_\chi^{-1} = \boldsymbol{\epsilon}\cdot\dot{\boldsymbol{\alpha}} \quad \text{with} \quad \dot{\boldsymbol{\alpha}} := \dot{\alpha}^k\,\boldsymbol{g}_k \circ \boldsymbol{\varphi}(\boldsymbol{X},t) \quad \text{where} \quad 2\,\mathbb{I}^{\text{skw}} := \boldsymbol{\epsilon}\cdot\boldsymbol{\epsilon} \tag{12}$$

Here, $\boldsymbol{\epsilon}$ denotes the third-order Levi-Civita tensor. Analogous to the orientation mapping, we herewith introduce a *rotation mapping* $\boldsymbol{\alpha} : \mathscr{B}_0 \times \mathscr{T} \to \mathbb{R}^{n_{\text{dim}}}$, which satisfies the condition $\boldsymbol{\alpha}(\boldsymbol{X},0) = \boldsymbol{0}$ at each point $\boldsymbol{X} \in \mathscr{B}_0$, where $\boldsymbol{0}$ designates the zero vector. We arrive at the reorientation dissipation

$$D_\chi^{\text{int}} := \left[\boldsymbol{N}_\chi - \boldsymbol{F}_\chi\,\boldsymbol{S}_\chi^t\right] : \boldsymbol{g}\,\dot{\boldsymbol{F}} - \boldsymbol{\tau}_\chi : \boldsymbol{\epsilon}\cdot\dot{\boldsymbol{\alpha}} \geq 0 \tag{13}$$

where we denote with $\boldsymbol{\tau}_\chi := \boldsymbol{F}\,\boldsymbol{S}_\chi\,\boldsymbol{F}_\chi^t$ a two-point orientational stress tensor, which we refer to as *orientational Kirchhoff stress tensor*. According to the Coleman-Noll procedure, we define the two-point *Piola reorientation stress tensor* $\boldsymbol{N}_\chi := \boldsymbol{F}_\chi\,\boldsymbol{S}_\chi^t$, where the *orientational stress tensor* $\boldsymbol{S}_\chi := \partial\Psi^{\text{ori}}/\partial\boldsymbol{C}_\chi$ is energy-conjugated to the tensor $\boldsymbol{C}_\chi$. Consequently, the reorientation dissipation D_χ^{int} is always non-negative with the equation

$$\boxed{-\frac{1}{2}\,\boldsymbol{\epsilon} : \boldsymbol{\tau}_\chi = \boldsymbol{\Sigma}_\chi} \quad \text{with} \quad \boldsymbol{\Sigma}_\chi = V_\chi\,\dot{\boldsymbol{\alpha}} \tag{14}$$

as local evolution equation, and takes the form of the bilinear form $D_\chi^{\text{int}} := 2\,\boldsymbol{\Sigma}_\chi\cdot\dot{\boldsymbol{\alpha}} \geq 0$. The parameter V_χ represents a *rotational viscosity parameter*. Therefore, we introduce the components α^k, $k = 1,\ldots,n_{\text{dim}}$, of the axial vector $\boldsymbol{\alpha}(\boldsymbol{X},t)$ as independent drilling degrees of freedom at each material point $\boldsymbol{X} \in \mathscr{B}_0$. The rotation of the orientation vector $\boldsymbol{n}_t$ owing to the reorientation in the LCE material is then given by the global equation

$$\dot{\boldsymbol{\chi}} = -\boldsymbol{\epsilon}\cdot\dot{\boldsymbol{\alpha}}\cdot\boldsymbol{\chi} \tag{15}$$

The natural constraint $\|\boldsymbol{n}_t\| = 1$ for the orientation vector at each point $\boldsymbol{x} \in \mathscr{B}_t$ is thus satisfied by the identity $\dot{\boldsymbol{\chi}}\cdot\boldsymbol{\chi} = 0$ at each time $t \in \mathscr{T}$ due to the condition $\boldsymbol{n}_0\cdot\boldsymbol{n}_0 = 1$.

2.2 Variational-based weak formulation

A well-known method for deriving a weak formulation is Galerkin's method. In this procedure, we require partial differential equations in advance, which are derived by balance laws as in [2]. But, in a dynamical framework, stable finite element methods in space and time are not straightforward with Galerkin's method, but they can be directly obtained by a *variational principle*. Balance laws and partial differential equations follow from the variational formulation and have not to be known in advance.

Therefore, in this paper, the goal is a variational-based weak formulation with independent (mixed) fields. Fields $\tilde{\boldsymbol{U}}_i$, $i = 1,\ldots,s$, whose time evolutions have to be continuous are introduced as time rates. Remainder independent fields $\tilde{\boldsymbol{V}}_j$, $j = 1,\ldots,p$, are temporally discontinuous, in general. The tilde sign highlights tensor fields as independent mixed fields. In this way, a discretization in space and time will be energy-consistent, if

the variational principle is based on the *total energy functional* $\mathcal{H}$ of the continuum. We choose the *mixed principle of virtual power* in Reference [3], which can be written as

$$\int_{t_n}^{t_{n+1}} \delta_* \dot{\mathcal{H}}(\dot{\tilde{\boldsymbol{U}}}_1, \dots \dot{\tilde{\boldsymbol{U}}}_s, \tilde{\boldsymbol{V}}_1, \dots \tilde{\boldsymbol{V}}_p)\, \mathrm{d}t = 0 \tag{16}$$

on any time step $\mathscr{T}_n := [t_n, t_{n+1}] \subset \mathscr{T}$ of time step size $h_n := t_{n+1} - t_n$. Since the variation δ is performed with respect to time derivatives of time functions $\tilde{\boldsymbol{U}}_i$ (δ_1 variations as in Jourdain's principle) as well as with respect to time functions $\tilde{\boldsymbol{V}}_j$ itself (δ or δ_0 variations as in D'Alembert's principle), we consider in the δ_* symbol the $*$ as a wild card.
We start by defining the virtual power $\delta_* \mathcal{P}_\varphi$ related with the deformation $\boldsymbol{\varphi}$, given by

$$\delta_* \mathcal{P}_\varphi := \delta_* \dot{\mathcal{T}}_\varphi(\dot{\boldsymbol{\varphi}}, \dot{\boldsymbol{v}}, \dot{\boldsymbol{p}}) + \delta_* \dot{\Pi}^{\mathrm{ext}}_\varphi(\dot{\boldsymbol{\varphi}}, \tilde{\boldsymbol{R}}) + \delta_* \dot{\Pi}^{\mathrm{int}}_\varphi(\dot{\boldsymbol{\varphi}}, \dot{\tilde{\boldsymbol{F}}}, \dot{\tilde{\boldsymbol{C}}}, \tilde{\boldsymbol{P}}, \tilde{\boldsymbol{S}}) \tag{17}$$

The first term of Eq. (17), associated with the inertia of material points $\boldsymbol{X} \in \mathscr{B}_0$, reads

$$\delta_* \dot{\mathcal{T}}_\varphi(\dot{\boldsymbol{\varphi}}, \dot{\boldsymbol{v}}, \dot{\boldsymbol{p}}) := \int_{\mathscr{B}_0} \delta_* \dot{\boldsymbol{v}} \cdot [\rho_0 \boldsymbol{v} - \boldsymbol{p}]\, \mathrm{d}V + \int_{\mathscr{B}_0} \delta_* \dot{\boldsymbol{p}} \cdot [\dot{\boldsymbol{\varphi}} - \boldsymbol{v}]\, \mathrm{d}V + \int_{\mathscr{B}_0} \delta_* \dot{\boldsymbol{\varphi}} \cdot \dot{\boldsymbol{p}}\, \mathrm{d}V \tag{18}$$

Here, the velocity $\boldsymbol{v}$ and momentum vector $\boldsymbol{p}$ are introduced as independent (mixed) fields. The second term of Eq. (17) arises from the introduction of mechanical volume loads $\boldsymbol{B}$, traction loads $\bar{\boldsymbol{T}}$ and prescribed boundary displacements $\bar{\boldsymbol{\varphi}}$. Here, we obtain

$$\begin{aligned} \delta_* \dot{\Pi}^{\mathrm{ext}}_\varphi(\dot{\boldsymbol{\varphi}}, \tilde{\boldsymbol{R}}) := & - \int_{\mathscr{B}_0} \delta_* \dot{\boldsymbol{\varphi}} \cdot \boldsymbol{B}\, \mathrm{d}V - \int_{\partial_T \mathscr{B}_0} \delta_* \dot{\boldsymbol{\varphi}} \cdot \bar{\boldsymbol{T}}\, \mathrm{d}A \\ & - \int_{\partial_\varphi \mathscr{B}_0} \delta_* \tilde{\boldsymbol{R}} \cdot [\dot{\boldsymbol{\varphi}} - \dot{\bar{\boldsymbol{\varphi}}}]\, \mathrm{d}A - \int_{\partial_\varphi \mathscr{B}_0} \delta_* \dot{\boldsymbol{\varphi}} \cdot \tilde{\boldsymbol{R}}\, \mathrm{d}A \end{aligned} \tag{19}$$

where $\tilde{\boldsymbol{R}}$ denotes the reaction forces on the Dirichlet boundary $\partial_\varphi \mathscr{B}_0 := \partial \mathscr{B}_0 \setminus \partial_T \mathscr{B}_0$ disjunct with the Neumann boundary $\partial_T \mathscr{B}_0$. The third term of Eq. (17) takes the form $\delta_* \dot{\Pi}^{\mathrm{int}}_\varphi(\dot{\boldsymbol{\varphi}}, \dot{\tilde{\boldsymbol{F}}}, \dot{\tilde{\boldsymbol{C}}}, \tilde{\boldsymbol{P}}, \tilde{\boldsymbol{S}}) := \delta_* \mathcal{P}^{\mathrm{int}}_\varphi$ with

$$\begin{aligned} \delta_* \mathcal{P}^{\mathrm{int}}_\varphi := & \int_{\mathscr{B}_0} \delta_* \tilde{\boldsymbol{P}} : \left[\mathrm{Grad}[\dot{\boldsymbol{\varphi}}] - \dot{\tilde{\boldsymbol{F}}} \right] \mathrm{d}V + \frac{1}{2} \int_{\mathscr{B}_0} \delta_* \tilde{\boldsymbol{S}} : \left[\frac{\partial}{\partial t} \left(\tilde{\boldsymbol{F}}^t \tilde{\boldsymbol{F}} \right) - \dot{\tilde{\boldsymbol{C}}} \right] \mathrm{d}V \\ & + \int_{\mathscr{B}_0} \delta_* \dot{\tilde{\boldsymbol{C}}} : \left[\frac{\partial \Psi}{\partial \tilde{\boldsymbol{C}}} - \frac{1}{2} \tilde{\boldsymbol{S}} \right] \mathrm{d}V + \int_{\mathscr{B}_0} \delta_* \dot{\tilde{\boldsymbol{F}}} : \left[\tilde{\boldsymbol{F}}\, \tilde{\boldsymbol{S}} - \tilde{\boldsymbol{P}} \right] \mathrm{d}V + \int_{\mathscr{B}_0} \tilde{\boldsymbol{P}} : \mathrm{Grad}[\delta_* \dot{\boldsymbol{\varphi}}]\, \mathrm{d}V \end{aligned} \tag{20}$$

where $\tilde{\boldsymbol{P}}$ and $\tilde{\boldsymbol{S}}$ denote the independent fields of the first and second Piola-Kirchhoff stress tensor, respectively. Now, we present the virtual power associated with the orientation $\boldsymbol{\chi}$. We introduce the micro inertia of the mesogens by the *virtual orientational kinetic power*

$$\begin{aligned} \delta_* \dot{\mathcal{T}}_\chi(\dot{\boldsymbol{\chi}}, \dot{\boldsymbol{v}}_\chi, \dot{\boldsymbol{p}}_\chi) := & \int_{\mathscr{B}_0} \delta_* \dot{\boldsymbol{v}}_\chi \cdot \left(\rho_0 \left[(l_\chi^2 - l_0^2) \boldsymbol{A}_0 + l_0^2\, \boldsymbol{I} \right] \boldsymbol{v}_\chi - \boldsymbol{p}_\chi \right) \mathrm{d}V \\ & + \int_{\mathscr{B}_0} \delta_* \dot{\boldsymbol{p}}_\chi \cdot [\dot{\boldsymbol{\chi}} - \boldsymbol{v}_\chi]\, \mathrm{d}V + \int_{\mathscr{B}_0} \delta_* \dot{\boldsymbol{\chi}} \cdot \dot{\boldsymbol{p}}_\chi\, \mathrm{d}V \end{aligned} \tag{21}$$

We introduce volume loads $\boldsymbol{B}_\chi$ and boundary loads $\bar{\boldsymbol{W}}$ acting on the orientation $\boldsymbol{\chi}$ (see Fig. 1) by the *virtual orientational external power* $\delta_* \dot{\Pi}^{\mathrm{ext}}_\chi(\dot{\boldsymbol{\alpha}}, \dot{\boldsymbol{\chi}}, \tilde{\boldsymbol{Z}}, \tilde{\boldsymbol{\tau}}_n, \tilde{\boldsymbol{\nu}}) =: \delta_* \mathcal{P}^{\mathrm{ext}}_\chi$ with

$$\begin{aligned} \delta_* \mathcal{P}^{\mathrm{ext}}_\chi := & - \int_{\mathscr{B}_0} \delta_* \dot{\boldsymbol{\chi}} \cdot \boldsymbol{B}_\chi\, \mathrm{d}V - \int_{\partial_W \mathscr{B}_0} \delta_* \dot{\boldsymbol{\chi}} \cdot \bar{\boldsymbol{W}}\, \mathrm{d}A - \int_{\partial_\chi \mathscr{B}_0} \delta_* \tilde{\boldsymbol{Z}} \cdot [\dot{\boldsymbol{\chi}} - \dot{\bar{\boldsymbol{\chi}}}]\, \mathrm{d}A - \int_{\partial_\chi \mathscr{B}_0} \delta_* \dot{\boldsymbol{\chi}} \cdot \tilde{\boldsymbol{Z}}\, \mathrm{d}A \\ & - \int_{\partial_\chi \mathscr{B}_0} 2\, \delta_* \tilde{\boldsymbol{\tau}}_n \cdot \tilde{\boldsymbol{\nu}}\, \mathrm{d}A - \int_{\partial_\chi \mathscr{B}_0} 2\, \delta_* \tilde{\boldsymbol{\nu}} \cdot \tilde{\boldsymbol{\tau}}_n\, \mathrm{d}A + \int_{\mathscr{B}_0} 2\, \delta_* \dot{\boldsymbol{\alpha}} \cdot \boldsymbol{\Sigma}_\chi\, \mathrm{d}V \end{aligned} \tag{22}$$

The volume loads $\boldsymbol{B}_\chi$ model a penetrating action on the mesogens in each material point $\boldsymbol{x} \in \mathscr{B}_t$, whereas the loads $\bar{\boldsymbol{W}}$ on the Neumann boundary $\partial_W \mathscr{B}_0$ model a non-penetrating action only on the outer mesogens. For the sake of completeness, we also introduce a prescribed orientation $\bar{\boldsymbol{\chi}}$ on the disjunct Dirichlet boundary $\partial_\chi \mathscr{B}_0 := \partial \mathscr{B}_0 \setminus \partial_W \mathscr{B}_0$. The last term denotes the *virtual internal reorientation dissipation*. Finally, the functional form of the *virtual orientational internal power* is given by

$$\delta_* \dot{\Pi}^{\text{int}}_\chi(\dot{\boldsymbol{\alpha}}, \dot{\boldsymbol{\chi}}, \dot{\tilde{\boldsymbol{F}}}, \dot{\tilde{\boldsymbol{F}}}_\chi, \dot{\tilde{\boldsymbol{G}}}_\chi, \dot{\tilde{\boldsymbol{C}}}_\chi, \dot{\tilde{\boldsymbol{K}}}_\chi, \tilde{\boldsymbol{\tau}}_n, \tilde{\boldsymbol{P}}_\chi, \tilde{\boldsymbol{P}}_K, \tilde{\boldsymbol{S}}_\chi, \tilde{\boldsymbol{S}}_K) := \delta_* \mathcal{P}^{\text{int}}_\chi \tag{23}$$

where

$$\begin{aligned}
\delta_* \mathcal{P}^{\text{int}}_\chi \;:=\; & \int_{\mathscr{B}_0} \delta_* \dot{\tilde{\boldsymbol{F}}} : \left[\tilde{\boldsymbol{F}}_\chi \, \tilde{\boldsymbol{S}}^t_\chi + \tilde{\boldsymbol{G}}_\chi \, \tilde{\boldsymbol{S}}^t_K \right] \mathrm{d}V + \int_{\mathscr{B}_0} 2\, \delta_* \tilde{\boldsymbol{\tau}}_n \cdot [\dot{\boldsymbol{\chi}} + \boldsymbol{\epsilon} \cdot \dot{\boldsymbol{\alpha}} \cdot \boldsymbol{\chi}] \, \mathrm{d}V \\
& + \int_{\mathscr{B}_0} \delta_* \tilde{\boldsymbol{P}}_\chi : \left[\dot{\boldsymbol{\chi}} \otimes \boldsymbol{n}_0 - \dot{\tilde{\boldsymbol{F}}}_\chi \right] \mathrm{d}V + \int_{\mathscr{B}_0} \delta_* \tilde{\boldsymbol{P}}_K : \left[\mathrm{Grad}[\dot{\boldsymbol{\chi}}] - \dot{\tilde{\boldsymbol{G}}}_\chi \right] \mathrm{d}V \\
& + \int_{\mathscr{B}_0} \delta_* \tilde{\boldsymbol{S}}_\chi : \left[\frac{\partial}{\partial t} \left(\tilde{\boldsymbol{F}}^t \tilde{\boldsymbol{F}}_\chi \right) - \dot{\tilde{\boldsymbol{C}}}_\chi \right] \mathrm{d}V + \int_{\mathscr{B}_0} \delta_* \tilde{\boldsymbol{S}}_K : \left[\frac{\partial}{\partial t} \left(\tilde{\boldsymbol{F}}^t \tilde{\boldsymbol{G}}_\chi \right) - \dot{\tilde{\boldsymbol{K}}}_\chi \right] \mathrm{d}V \\
& + \int_{\mathscr{B}_0} \delta_* \dot{\tilde{\boldsymbol{C}}}_\chi : \left[\frac{\partial \Psi}{\partial \tilde{\boldsymbol{C}}_\chi} - \tilde{\boldsymbol{S}}_\chi \right] \mathrm{d}V + \int_{\mathrm{B}_0} \delta_* \dot{\tilde{\boldsymbol{K}}}_\chi : \left[\frac{\partial \Psi}{\partial \tilde{\boldsymbol{K}}_\chi} - \tilde{\boldsymbol{S}}_K \right] \mathrm{d}V \\
& + \int_{\mathscr{B}_0} \delta_* \dot{\tilde{\boldsymbol{F}}}_\chi : \left[\tilde{\boldsymbol{F}} \, \tilde{\boldsymbol{S}}_\chi - \tilde{\boldsymbol{P}}_\chi \right] \mathrm{d}V + \int_{\mathscr{B}_0} \delta_* \dot{\tilde{\boldsymbol{G}}}_\chi : \left[\tilde{\boldsymbol{F}} \, \tilde{\boldsymbol{S}}_K - \tilde{\boldsymbol{P}}_K \right] \mathrm{d}V \\
& + \int_{\mathscr{B}_0} \tilde{\boldsymbol{P}}_\chi : [\delta_* \dot{\boldsymbol{\chi}} \otimes \boldsymbol{n}_0] \, \mathrm{d}V + \int_{\mathrm{B}_0} \tilde{\boldsymbol{P}}_K : \mathrm{Grad}[\delta_* \dot{\boldsymbol{\chi}}] \, \mathrm{d}V \\
& + \int_{\mathscr{B}_0} \left[\frac{1}{2} \, \boldsymbol{\epsilon} : \boldsymbol{\tau}_\chi - \tilde{\boldsymbol{\tau}}_n \cdot \boldsymbol{\epsilon} \cdot \boldsymbol{\chi} \right] \cdot 2\, \delta_* \dot{\boldsymbol{\alpha}} \, \mathrm{d}V + \int_{\mathscr{B}_0} 2\, \tilde{\boldsymbol{\tau}}_n \cdot \delta_* \dot{\boldsymbol{\chi}} \, \mathrm{d}V
\end{aligned}$$

We obtain $\tilde{\boldsymbol{S}}_\chi$ as Lagrange multiplier of the weak definition of $\tilde{\boldsymbol{C}}_\chi$. This weak definition of strain and stress tensors guarantees the energy-consistent time integration [3]. In the same way, we introduce the *distorsion stress tensor* $\tilde{\boldsymbol{S}}_K$ energy-conjugated to $\tilde{\boldsymbol{K}}_\chi$. Further, weakly defined stress tensors are $\boldsymbol{P}_\chi := \boldsymbol{F}\, \boldsymbol{S}_\chi$ and $\boldsymbol{P}_K := \boldsymbol{F}\, \boldsymbol{S}_K$, which we refer to as *Piola orientational stress* and *Piola distorsion stress*, respectively. The vector field $2\,\boldsymbol{\tau}_n$ is the Lagrange multiplier of Eq. (15). We call this vector the *rotation stress vector*.
The weak forms of the considered continuum problem arise from the application of the variational principle in Eq. (16) to the virtual power functional

$$\boxed{\delta_* \dot{\mathcal{H}} := \delta_* \mathcal{P}_\varphi + \delta_* \dot{\mathcal{T}}_\chi(\dot{\boldsymbol{\chi}}, \dot{\boldsymbol{v}}_\chi, \dot{\boldsymbol{p}}_\chi) + \delta_* \mathcal{P}^{\text{ext}}_\chi + \delta_* \mathcal{P}^{\text{int}}_\chi} \tag{24}$$

We obtain three main weak forms coupled in the deformation $\boldsymbol{\varphi}$, the orientation $\boldsymbol{\chi}$ and the rotation stress vector field $2\,\boldsymbol{\tau}_n$. We solve these weak forms with a monolithic solution strategy. The deformation $\boldsymbol{\varphi}$ is determined by the *weak balance of linear momentum*

$$\begin{aligned}
& \int_{\mathscr{T}_n} \int_{\mathscr{B}_0} \delta_* \dot{\boldsymbol{\varphi}} \cdot [\dot{\boldsymbol{p}} - \boldsymbol{B}] \, \mathrm{d}V \mathrm{d}t \; - \int_{\mathscr{T}_n} \int_{\partial_T \mathscr{B}_0} \bar{\boldsymbol{T}} \cdot \delta_* \dot{\boldsymbol{\varphi}} \, \mathrm{d}A \, \mathrm{d}t \\
& + \int_{\mathscr{T}_n} \int_{\mathscr{B}_0} \tilde{\boldsymbol{P}} : \mathrm{Grad}[\delta_* \dot{\boldsymbol{\varphi}}] \, \mathrm{d}V \mathrm{d}t \; = \int_{\mathscr{T}_n} \int_{\partial_\varphi \mathscr{B}_0} \tilde{\boldsymbol{R}} \cdot \delta_* \dot{\boldsymbol{\varphi}} \, \mathrm{d}A \, \mathrm{d}t
\end{aligned} \tag{25}$$

The rotation stress $2\,\boldsymbol{\tau}_n$ is associated with the *weak balance of orientational momentum*

$$\begin{aligned}
& \int_{\mathscr{T}_n} \int_{\mathscr{B}_0} \delta_* \dot{\boldsymbol{\chi}} \cdot \left[\dot{\boldsymbol{p}}_\chi + 2\, \tilde{\boldsymbol{\tau}}_n - \boldsymbol{B}_\chi \right] \mathrm{d}V \mathrm{d}t - \int_{\mathscr{T}_n} \int_{\partial_W \mathscr{B}_0} \bar{\boldsymbol{W}} \cdot \delta_* \dot{\boldsymbol{\chi}} \, \mathrm{d}A \, \mathrm{d}t \\
& + \int_{\mathscr{T}_n} \int_{\mathscr{B}_0} \tilde{\boldsymbol{P}}_K : \mathrm{Grad}[\delta_* \dot{\boldsymbol{\chi}}] \, \mathrm{d}V \mathrm{d}t + \int_{\mathscr{T}_n} \int_{\mathscr{B}_0} \tilde{\boldsymbol{P}}_\chi : [\delta_* \dot{\boldsymbol{\chi}} \otimes \boldsymbol{n}_0] \, \mathrm{d}V \mathrm{d}t = \int_{\mathscr{T}_n} \int_{\partial_\chi \mathscr{B}_0} \tilde{\boldsymbol{Z}} \cdot \delta_* \dot{\boldsymbol{\chi}} \, \mathrm{d}A \, \mathrm{d}t
\end{aligned} \tag{26}$$

Table 1: Energy and momentum functions of the LCE extended continuum.

Kinetic energy $\mathcal{T}(t) := \int_{\mathscr{B}_0} \frac{1}{2}\, \boldsymbol{v} \cdot \boldsymbol{p}\, \mathrm{d}V$	Kinetic energy of orientation $\mathcal{T}_\chi(t) := \int_{\mathscr{B}_0} \frac{1}{2}\, \boldsymbol{v}_\chi \cdot \boldsymbol{p}_\chi\, \mathrm{d}V$	Potential energy $\mathit{\Pi}^{\mathrm{int}}(t) := \int_{\mathscr{B}_0} \Psi\, \mathrm{d}V$
Linear momentum $\boldsymbol{L}(t) := \int_{\mathscr{B}_0} \boldsymbol{p}\, \mathrm{d}V$	Angular momentum $\boldsymbol{J}(t) := \int_{\mathscr{B}_0} \boldsymbol{\varphi} \times \boldsymbol{p}\, \mathrm{d}V$	Momentum of orientation $\boldsymbol{L}_\chi(t) := \int_{\mathscr{B}_0} \boldsymbol{p}_\chi\, \mathrm{d}V$
Moment of momentum $\boldsymbol{J}_\chi(t) := \int_{\mathscr{B}_0} \boldsymbol{\chi} \times \boldsymbol{p}_\chi\, \mathrm{d}V$	Reorientation function $\mathcal{C}^{\mathrm{ori}}(t) := \int_{\mathscr{B}_0} \left[\|\boldsymbol{\chi}\|^2 - 1\right] \mathrm{d}V$	Total energy $\mathcal{H} := \mathcal{T} + \mathcal{T}_\chi + \mathit{\Pi}^{\mathrm{int}} + \mathit{\Pi}^{\mathrm{ext}}$

Finally, the orientation $\boldsymbol{\chi}$ or the orientation vector $\boldsymbol{n}_t$, respectively, is determined by the *weak balance of orientation rate vector*

$$\int_{\mathscr{T}_n}\int_{\mathscr{B}_0} 2\,\delta_*\tilde{\boldsymbol{\tau}}_n \cdot [\dot{\boldsymbol{\chi}} + \boldsymbol{\epsilon} \cdot \dot{\boldsymbol{\alpha}} \cdot \boldsymbol{\chi}]\, \mathrm{d}V\mathrm{d}t \;=\; \int_{\mathscr{T}_n}\int_{\partial_\chi \mathscr{B}_0} 2\,\delta_*\tilde{\boldsymbol{\tau}}_n \cdot \tilde{\boldsymbol{\nu}}\, \mathrm{d}A\, \mathrm{d}t \tag{27}$$

The vector field $\tilde{\boldsymbol{\nu}}$ represents a reaction due to a prescribed orientation on the boundary $\partial_\chi \mathscr{B}_0$. We refer to this vector field as *reaction velocity field*. The local evolution equation in Eq. (14) is solved on the element level with an elementwise space approximation and a consistent linearisation as the finite viscoelasticity in Reference [3].

2.3 Balance laws

The weak formulation in Section 2.2 satisfies different balance laws associated with energy and momentum functions defined in Tab. 1 in consequence of symmetry properties of the time evolutions pertaining to $\boldsymbol{\varphi}$, $\boldsymbol{\chi}$ and $\tilde{\boldsymbol{\tau}}_n$ with respect to Euclidean transformations. Therefore, by choosing specific variations as test functions, we obtain balance laws.
First, the *balance law of linear momentum* describes a symmetry of the LCE material with respect to virtual translations along a constant vector $\boldsymbol{c} \in \mathbb{R}^{n_{\mathrm{dim}}}$. This balance law is obtained by choosing the test function $\delta_*\dot{\boldsymbol{\varphi}} = \boldsymbol{c}$, leading to

$$\boldsymbol{L}(t_{n+1}) - \boldsymbol{L}(t_n) = \int_{\mathscr{T}_n}\int_{\mathscr{B}_0} \boldsymbol{B}\, \mathrm{d}V\mathrm{d}t \;+ \int_{\mathscr{T}_n}\int_{\partial_T \mathscr{B}_0} \bar{\boldsymbol{T}}\, \mathrm{d}A\, \mathrm{d}t \;+ \int_{\mathscr{T}_n}\int_{\partial_\varphi \mathscr{B}_0} \tilde{\boldsymbol{R}}\, \mathrm{d}A\, \mathrm{d}t \tag{28}$$

In the same way, we obtain a *balance law of orientational momentum* by choosing the test function $\delta_*\dot{\boldsymbol{\chi}} = \boldsymbol{c}$, where $\boldsymbol{c} \in \mathbb{R}^{n_{\mathrm{dim}}}$ denotes any constant orientation. We arrive at

$$\boldsymbol{L}_\chi(t_{n+1}) - \boldsymbol{L}_\chi(t_n) = \int_{\mathscr{T}_n}\int_{\mathscr{B}_0} [\boldsymbol{B}_\chi - 2\,\tilde{\boldsymbol{\tau}}_n - \tilde{\boldsymbol{P}}_\chi\, \boldsymbol{n}_0]\, \mathrm{d}V\mathrm{d}t \;+ \int_{\mathscr{T}_n}\int_{\partial_\chi \mathscr{B}_0} \bar{\boldsymbol{W}}\, \mathrm{d}A\, \mathrm{d}t \;+ \int_{\mathscr{T}_n}\int_{\partial_\chi \mathscr{B}_0} \tilde{\boldsymbol{Z}}\, \mathrm{d}A\, \mathrm{d}t \tag{29}$$

A further symmetry property of the deformation $\boldsymbol{\varphi}$ is associated with a virtual rotation of the LCE material around a constant axial vector $\boldsymbol{c} \in \mathbb{R}^{n_{\mathrm{dim}}}$, introduced by the test function $\delta_*\dot{\boldsymbol{\varphi}} = \boldsymbol{c} \times \boldsymbol{\varphi}$. Here, we apply the definition $\boldsymbol{t}_1 \times \boldsymbol{t}_2 := \boldsymbol{\epsilon} : [\boldsymbol{t}_1 \otimes \boldsymbol{t}_2]$ of the cross product of two vectors $\boldsymbol{t}_1$ and $\boldsymbol{t}_2$. This *balance law of angular momentum* is given by

$$\begin{aligned} \boldsymbol{J}(t_{n+1}) - \boldsymbol{J}(t_n) \;&=\; \int_{\mathscr{T}_n}\int_{\mathscr{B}_0} \boldsymbol{\varphi} \times \boldsymbol{B}\, \mathrm{d}V\mathrm{d}t + \int_{\mathscr{T}_n}\int_{\partial_T \mathscr{B}_0} \boldsymbol{\varphi} \times \bar{\boldsymbol{T}}\, \mathrm{d}A\, \mathrm{d}t + \int_{\mathscr{T}_n}\int_{\partial_\varphi \mathscr{B}_0} \boldsymbol{\varphi} \times \tilde{\boldsymbol{R}}\, \mathrm{d}A\, \mathrm{d}t \\ &+ \int_{\mathscr{T}_n}\int_{\mathscr{B}_0} [\tilde{\boldsymbol{F}}_\chi \tilde{\boldsymbol{S}}^t_\chi + \tilde{\boldsymbol{G}}_\chi \tilde{\boldsymbol{S}}^t_K] \times \tilde{\boldsymbol{F}}\, \mathrm{d}V\mathrm{d}t \end{aligned} \tag{30}$$

by taking into account the cross product $\boldsymbol{T}_1 \times \boldsymbol{T}_2 := \boldsymbol{\epsilon} : [\boldsymbol{T}_1 \cdot \boldsymbol{T}_2^t]$ of two second-order tensors $\boldsymbol{T}_1$ and $\boldsymbol{T}_2$. Without introducing an orientation vector $\boldsymbol{n}_t$, the last term in Eq. (30) vanishes due to the symmetry property $\tilde{\boldsymbol{P}}\tilde{\boldsymbol{F}}^t = \tilde{\boldsymbol{F}}\tilde{\boldsymbol{P}}^t$. But, bearing in mind the rotation of the orientation vector $\boldsymbol{n}_t$ during reorientations, we obtain distributed couples.
Analogous to the angular momentum balance law, the test function $\delta_*\dot{\boldsymbol{\chi}} = \boldsymbol{c} \times \boldsymbol{\chi}$ leads to a balance law associated with a virtual rotation of the orientation vector around any direction $\boldsymbol{c} \in \mathbb{R}^{n_{\mathrm{dim}}}$. This *balance law of moment of orientational momentum* reads

$$\begin{aligned}\boldsymbol{J}_\chi(t_{n+1}) - \boldsymbol{J}_\chi(t_n) = &\int_{\mathscr{T}_n}\int_{\mathscr{B}_0} \boldsymbol{\chi} \times \boldsymbol{B}_\chi \,\mathrm{d}V\mathrm{d}t + \int_{\mathscr{T}_n}\int_{\partial_W\mathscr{B}_0} \boldsymbol{\chi} \times \bar{\boldsymbol{W}} \,\mathrm{d}A\,\mathrm{d}t + \int_{\mathscr{T}_n}\int_{\partial_\chi\mathscr{B}_0} \boldsymbol{\chi} \times \tilde{\boldsymbol{Z}} \,\mathrm{d}A\,\mathrm{d}t \\ &- \int_{\mathscr{T}_n}\int_{\mathscr{B}_0} [\tilde{\boldsymbol{F}}_\chi \tilde{\boldsymbol{S}}_\chi^t + \tilde{\boldsymbol{G}}_\chi \tilde{\boldsymbol{S}}_K^t] \times \tilde{\boldsymbol{F}} \,\mathrm{d}V\mathrm{d}t - \int_{\mathscr{T}_n}\int_{\mathscr{B}_0} \boldsymbol{\chi} \times 2\,\tilde{\boldsymbol{\tau}}_n \,\mathrm{d}V\mathrm{d}t \end{aligned} \tag{31}$$

All distributed couples in the LCE material are eliminated by adding Eqs. (30) and (31), with exept of the couples $\boldsymbol{\chi} \times 2\,\tilde{\boldsymbol{\tau}}_n$ generated by the normalized reorientation of $\boldsymbol{n}_t$.
Second, we obtain energy balance laws as symmetry with respect to virtual translations along the time axis. Choosing $\delta_*\dot{\boldsymbol{\varphi}} = \dot{\boldsymbol{\varphi}}$, we obtain the *balance law of kinetic energy*

$$\begin{aligned}\mathcal{T}(t_{n+1}) - \mathcal{T}(t_n) = &\int_{\mathscr{T}_n}\int_{\mathscr{B}_0} \boldsymbol{B} \cdot \dot{\boldsymbol{\varphi}} \,\mathrm{d}V\mathrm{d}t + \int_{\mathscr{T}_n}\int_{\partial_T\mathscr{B}_0} \bar{\boldsymbol{T}} \cdot \dot{\boldsymbol{\varphi}} \,\mathrm{d}A\,\mathrm{d}t + \int_{\mathscr{T}_n}\int_{\partial_\varphi\mathscr{B}_0} \tilde{\boldsymbol{R}} \cdot \dot{\boldsymbol{\varphi}} \,\mathrm{d}A\,\mathrm{d}t \\ &- \int_{\mathscr{T}_n}\int_{\mathscr{B}_0} [\tilde{\boldsymbol{S}} : \dot{\tilde{\boldsymbol{F}}}^t\tilde{\boldsymbol{F}} + \tilde{\boldsymbol{S}}_\chi : \dot{\tilde{\boldsymbol{F}}}^t\tilde{\boldsymbol{F}}_\chi + \tilde{\boldsymbol{S}}_K : \dot{\tilde{\boldsymbol{F}}}^t\tilde{\boldsymbol{G}}_\chi] \,\mathrm{d}V\mathrm{d}t \end{aligned} \tag{32}$$

depending on external loads, but also on the stress power in the LCE material. Since we assume a micro inertia of the mesogens, we also obtain a *balance law of orientational kinetic energy* by inserting the test function $\delta_*\dot{\boldsymbol{\chi}} = \dot{\boldsymbol{\chi}}$. This leads to the relation

$$\begin{aligned}\mathcal{T}_\chi(t_{n+1}) - \mathcal{T}_\chi(t_n) = &\int_{\mathscr{T}_n}\int_{\mathscr{B}_0} \boldsymbol{B}_\chi \cdot \dot{\boldsymbol{\chi}} \,\mathrm{d}V\mathrm{d}t + \int_{\mathscr{T}_n}\int_{\partial_\varphi\mathscr{B}_0} \bar{\boldsymbol{W}} \cdot \dot{\boldsymbol{\chi}} \,\mathrm{d}A\,\mathrm{d}t + \int_{\mathscr{T}_n}\int_{\partial_\varphi\mathscr{B}_0} \tilde{\boldsymbol{Z}} \cdot \dot{\boldsymbol{\chi}} \,\mathrm{d}A\,\mathrm{d}t \\ &- \int_{\mathscr{T}_n}\int_{\mathscr{B}_0} [\tilde{\boldsymbol{S}}_\chi : \tilde{\boldsymbol{F}}^t \left(\dot{\tilde{\boldsymbol{F}}}_\chi + \boldsymbol{\epsilon} \cdot \dot{\boldsymbol{\alpha}} \cdot \tilde{\boldsymbol{F}}_\chi\right) + \tilde{\boldsymbol{S}}_K : \tilde{\boldsymbol{F}}^t\dot{\tilde{\boldsymbol{G}}}_\chi + D_\chi^{\mathrm{int}}] \,\mathrm{d}V\mathrm{d}t \end{aligned} \tag{33}$$

by taking into account the *variational form* of the evolution equation in Eq. (14).
The *potential energy balance law* of a continuum follows from the time derivative of the total potential energy $\mathit{\Pi} := \mathit{\Pi}^{\mathrm{int}} + \mathit{\Pi}^{\mathrm{ext}}$, and is the consequence of a path-independent material and loads. In this paper, we apply path-independent volume dead loads, such that we obtain the *external potential energy*

$$\mathit{\Pi}^{\mathrm{ext}}(t) := -\int_{\mathscr{B}_0} \boldsymbol{B} \cdot \boldsymbol{\varphi} \,\mathrm{d}V\mathrm{d}t - \int_{\mathscr{B}_0} \boldsymbol{B}_\chi \cdot \boldsymbol{\chi} \,\mathrm{d}V\mathrm{d}t \tag{34}$$

The time derivative $\dot{\mathit{\Pi}}$ of the potential energy then leads to the balance law

$$\begin{aligned}\mathit{\Pi}(t_{n+1}) - \mathit{\Pi}(t_n) = &\int_{\mathscr{T}_n}\int_{\mathscr{B}_0} [\tilde{\boldsymbol{S}}_\chi : \frac{\partial}{\partial t}\Big(\tilde{\boldsymbol{F}}^t\tilde{\boldsymbol{F}}_\chi\Big) + \tilde{\boldsymbol{S}}_K : \frac{\partial}{\partial t}\Big(\tilde{\boldsymbol{F}}^t\tilde{\boldsymbol{G}}_\chi\Big) + \tilde{\boldsymbol{S}}_\chi : \tilde{\boldsymbol{F}}^t(\boldsymbol{\epsilon} \cdot \dot{\boldsymbol{\alpha}})\tilde{\boldsymbol{F}}_\chi] \,\mathrm{d}V\mathrm{d}t \\ &+ \int_{\mathscr{T}_n}\int_{\mathscr{B}_0} \Big[\tilde{\boldsymbol{S}} : \dot{\tilde{\boldsymbol{F}}}^t\tilde{\boldsymbol{F}} - \boldsymbol{B} \cdot \dot{\boldsymbol{\varphi}} - \boldsymbol{B}_\chi \cdot \dot{\boldsymbol{\chi}}\Big] \,\mathrm{d}V\mathrm{d}t \end{aligned} \tag{35}$$

Accordingly, the presented reorientation formulation leads to the well-known *total energy balance law* by adding Eq. (32), Eq. (33) and Eq. (35), which coincides with the first law of thermodynamics depending only on the power of non-conservative loads *and* the

reorientation dissipation D_χ^{int}. This dissipation only vanishes in the total energy balance of a non-isothermal formulation, which is also analogous to finite thermo-viscoelasticity. The last balance law is the *balance law of reorientation* pertaining to the function $\mathcal{C}^{\text{ori}}$. Choosing the test function $\delta_*\tilde{\boldsymbol{\tau}}_n = \boldsymbol{\chi}$, we arrive at the balance law

$$\mathcal{C}^{\text{ori}}(t_{n+1}) - \mathcal{C}^{\text{ori}}(t_n) \equiv \int_{\mathscr{T}_n}\int_{\mathscr{B}_0} 2\,\boldsymbol{\chi}\cdot\dot{\boldsymbol{\chi}}\,\mathrm{d}V\,\mathrm{d}t = \int_{\mathscr{T}_n}\int_{\partial_\chi\mathscr{B}_0} 2\,\boldsymbol{\chi}\cdot\tilde{\boldsymbol{\nu}}\,\mathrm{d}A\,\mathrm{d}t \tag{36}$$

pertaining to the length of the orientation vector $\|\boldsymbol{n}_t\| = \|\boldsymbol{n}_0\| \equiv 1$ on each time step $\mathscr{T}_n$.

3 SPACE-TIME DISCRETIZATION

As in Reference [3], we introduce in Eq. (24) Galerkin time approximation polynomials with respect to the normalized time $\alpha(t) := (t - t_n)/h_n \in [0, 1]$ associated with $\mathscr{T}_n$. As mentioned above, in the time approximation, we distinguish between the time rate variables $\phi^n \in \{\boldsymbol{\varphi}^n, \boldsymbol{v}^n, \boldsymbol{p}^n, \tilde{\boldsymbol{F}}^n, \tilde{\boldsymbol{C}}^n, \boldsymbol{\chi}^n, \boldsymbol{v}_\chi^n, \boldsymbol{p}_\chi^n, \boldsymbol{\alpha}^n, \tilde{\boldsymbol{F}}_\chi^n, \tilde{\boldsymbol{G}}_\chi^n, \tilde{\boldsymbol{C}}_\chi^n, \tilde{\boldsymbol{K}}_\chi^n\}$ and the remainder mixed fields. A time rate variable field ϕ^n on the n-th time step $\mathscr{T}_n$ is approximated in time by k-order Lagrange polynomials $M_I(\alpha), I = 1, \ldots, k+1$. Then, we approximate the remainder mixed fields and variations $\tilde{\phi}^n$ on the n-th time step by $k-1$ order Lagrange polynomials $\tilde{M}_J(\alpha), J = 1, \ldots, k$, such that

$$\phi_\alpha^n := \sum_{I=1}^{k+1} M_I(\alpha)\,\phi_I^n \qquad\qquad \tilde{\phi}_\alpha^n := \sum_{J=1}^{k} \tilde{M}_J(\alpha)\,\tilde{\phi}_J^n \tag{37}$$

We temporally discretize the time integrals by a k-point Gaussian quadrature rule. In Eq. (24), we apply a *globally continuous* space discretization with hexahedral elements, based on local finite element shape functions $N_a(\boldsymbol{\zeta})$, $a = 1, \ldots, n_{\text{node}}$, defined on the parent domain $\mathscr{B}_\square := [-1, 1] \times [-1, 1] \times [-1, 1]$, and the associated quadrature rules to the fields $\Phi \in \{\boldsymbol{\varphi}, \boldsymbol{v}, \boldsymbol{p}, \tilde{\boldsymbol{R}}, \boldsymbol{\chi}, \boldsymbol{v}_\chi, \boldsymbol{p}_\chi, \tilde{\boldsymbol{\tau}}_n, \tilde{\boldsymbol{Z}}, \tilde{\boldsymbol{\nu}}, \delta_*\dot{\boldsymbol{\varphi}}, \delta_*\dot{\boldsymbol{v}}, \delta_*\dot{\boldsymbol{p}}, \delta_*\tilde{\boldsymbol{R}}, \delta_*\dot{\boldsymbol{\chi}}, \delta_*\dot{\boldsymbol{v}}_\chi, \delta_*\dot{\boldsymbol{p}}_\chi, \delta_*\tilde{\boldsymbol{\tau}}_n, \delta_*\tilde{\boldsymbol{Z}}, \delta_*\tilde{\boldsymbol{\nu}}\}$. Remainder fields $\hat{\Phi}$ on the e-th finite element are *globally discontinuously* approximated in space by local finite element shape functions $\hat{N}_b(\boldsymbol{\zeta})$, $b = 1, \ldots, \hat{n}_{\text{node}}$, *well-defined* on the domain $\mathscr{B}_\square$, so that on the e-th finite element in space, $e = 1, \ldots, n_{\text{el}}$, we apply

$$\Phi_{\boldsymbol{\zeta}}^e := \sum_{a=1}^{n_{\text{node}}} N_a(\boldsymbol{\zeta})\,\Phi_a^e \qquad\qquad \hat{\Phi}_{\boldsymbol{\zeta}}^e := \sum_{b=1}^{\hat{n}_{\text{node}}} \hat{N}_b(\boldsymbol{\zeta})\,\hat{\Phi}_b^e \tag{38}$$

The local shape functions $\hat{N}_b(\boldsymbol{\zeta})$, $b = 1, \ldots, \hat{n}_{\text{node}}$, also fulfill a completeness condition. Motivated by Reference [8], we apply for $\boldsymbol{\alpha}$ and $\delta_*\dot{\boldsymbol{\alpha}}$ local finite element shape functions $\tilde{N}_c(\boldsymbol{\zeta})$, $c = 1, \ldots, \tilde{n}_{\text{node}}$, which are generally different from $N_a(\boldsymbol{\zeta})$ and $\hat{N}_b(\boldsymbol{\zeta})$. In order to satisfy the property in Eq. (35) also in a discrete sense, we extend the stress approximations (cp. [3]). Further, we implemented the dyadic product $\dot{\boldsymbol{\chi}} \otimes \boldsymbol{n}_0$ in a special way, such that a special $\bar{B}$-operator has arisen. We report about these details in a follow up paper.

4 NUMERICAL EXAMPLE

As summarized in Section 2.3, the reorientation of the mesogens or the orientation vectors, respectively, directly affects the deformation of a continuum body. This is obvious by a closer inspection of the balance laws. The balance law of linear momentum is not influenced by the Frank free energy and the interactive free energy, whereas in the balance

law of angular momentum, we obtain distributed couples which affects the motion. Since the reorientation process is dissipative, we obtain a decreasing total energy due to the internal reorientation dissipation. In order to demonstrate this behaviour, we initiate a free rotation of a thin strip of LCE material ($0.3 \times 12.5 \times 75$ [mm]). The rotation around the center of mass is initiated with an initial angular velocity $\omega = 32$ [1/s] around the z-axis. In Fig. 2, we compare this motion without (left) and with (right) reorientation. Without a dissipative reorientation, the strip steadily rotates as expected anti-clockwise in the $x-y$-plane and the momenta and total energy are conserved. However, the distributed couples of reorientation leads to an unsteady right-left-rotation with large deformations, and the reorientation dissipation D_χ^{int} leads to a decreasing total energy.

5 CONCLUSIONS

The reorientation of the mesogens can be formulated by a variational principle as a dissipative process analogous to finite thermo-viscoelasticty. Therefore, the extention of the present formulation to the non-isothermal framework is possible and the next step.

Acknowledgements. This research is provided by the 'Deutsche Forschungsgemeinschaft' (DFG) under the grant GR 3297/7-1. This support is gratefully acknowledged.

REFERENCES

[1] Corbett, D. and Warner, M. Changing liquid crystal elastomer ordering with light–a route to opto-mechanically responsive materials. *Liquid Crystals* (2009) **36**:1263–1280.

[2] Anderson, D.R.; Carlson, D.E. and Fried, E. A continuum-mechanical theory for nematic elastomers. *Journal of Elasticity* (1999) **56**:33–58.

[3] Groß, M.; Dietzsch, J. and Röbiger, C. Non-isothermal energy–momentum time integrations with drilling degrees of freedom of composites with viscoelastic fiber bundles and curvature–twist stiffness. *Comput. Methods Appl. Mech. Engrg.* (2020) **365**:112973.

[4] Frank, F.C. I. Liquid crystals. On the theory of liquid crystals. *Discuss. Faraday Soc.* (1958) **25**:19–28.

[5] Leslie, F.M. Some constitutive equations for liquid crystals. *Archive for Rational Mechanics and Analysis* (1968) **28**(4):265–283.

[6] De Luca, M.; DeSimone, A.; Petelin, A. and Čopič M. Sub-stripe pattern formation in liquid crystal elastomers: Experimental observations and numerical simulations. *J. Mech. Phys. Solids* (2013) **61**(11):2161–2177.

[7] Himpel, G.; Menzel, A.; Kuhl, E. and Steinmann P. Time-dependent fibre reorientation of transversely isotropic continua—Finite element formulation and consistent linearization. *Int. J. Numer. Methods Eng.*, (2008) **73**(10):1413–1433.

[8] Ibrahimbegovic, A. and Wilson, E. L. Thick shell and solid finite elements with independent rotation fields. *Int. J. Numer. Methods Eng.*, (1991) **31**(7):1393–1414.

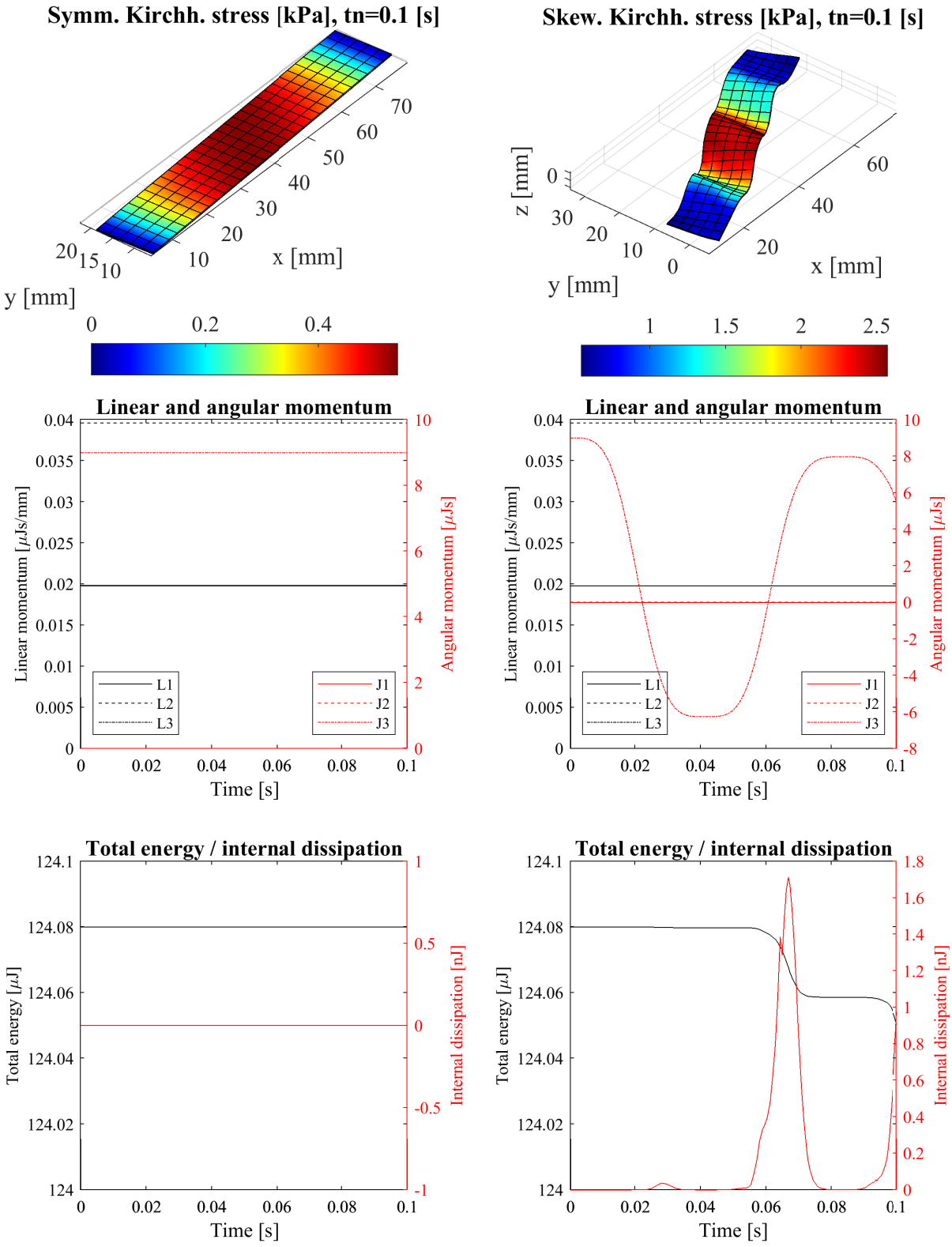

Figure 2: Comparison of time evolutions without (left) and with (right) reorientation. As in [3], N_a belongs to a 20-node serendibity hexahedral element (H20) and $\hat{N}_b$ to a 12-node prismatic element (P12). Motivated by [8], $\tilde{N}_c$ belongs to a 8-node Lagrangian hexahedral element (H8). Colours in the left top plot indicate the Kirchhoff stress $\boldsymbol{\tau} = \tilde{\boldsymbol{P}}\tilde{\boldsymbol{F}}^t$, where in the right, finite elements are coloured by the skew-symmetric part of $\boldsymbol{\tau}_\chi$. The LCE material is defined by polyconvex free energy functions with $\rho_0 = 0.00176\,[\mathrm{g/mm^3}]$, $V_\chi = 1\,[\mathrm{kPa}\cdot\mathrm{s}]$, Young's modulus $E \approx 0.914\,[\mathrm{MPa}]$, Poisson's ratio $\nu \approx 0.493$. Further, the initial orientation $\boldsymbol{n}_0 = \boldsymbol{e}_y$ is used.